Strengthening contrast between precipitation in tropical wet and dry regions

AGU PUBLICATIONS

Geophysical Research Letters

RESEARCH LETTER
10.1002/2016GL071194

Key Points:
- Tracking wet and dry regions as they shift over time and vary in models and observations shows precipitation changes follow the WWDD theory
- The WWDD signal is reduced and disappears in model dry regions, when they are not tracked over time in each simulation
- Tracking regions significantly improves agreement between models of future changes and between observations and models of past changes

Supporting Information:
- Supporting Information S1

Correspondence to:
D. Polson,
dpolson@staffmail.ed.ac.uk

Citation:
Polson, D., and G. Hegerl (2016), Strengthening contrast between precipitation in tropical wet and dry regions, *Geophys. Res. Lett.*, *43*, doi:10.1002/2016GL071194.

Received 24 SEP 2016
Accepted 10 DEC 2016
Accepted article online 15 DEC 2016

Strengthening contrast between precipitation in tropical wet and dry regions

D. Polson[1] and G. C. Hegerl[1]

[1] School of GeoSciences, University of Edinburgh, Crew Building, Edinburgh, UK

Abstract The wet-gets-wetter, dry-gets-drier paradigm (WWDD) is widely used to summarize the expected response of the hydrological cycle to global warming. While some studies find that changes in observations and climate models support the WWDD paradigm, others find that it is more complicated at local scales and over land. This discrepancy is partly explained by differences in model climatologies and by movement of the wet and dry regions. Here we show that by tracking changes in wet and dry regions as they shift over the tropics and vary in models, mean precipitation changes follow the WWDD pattern in observations and models over land and ocean. However, this signal is reduced and disappears in model dry regions, when these factors are not accounted for. Accounting for seasonal and interannual shifts of the regions and climatological differences between models reduces uncertainty in predictions of future precipitation changes and makes these changes detectable earlier.

1. Introduction

Underlying the wet-gets-wetter, dry-gets-drier paradigm are well-understood physical mechanisms related to the intensification of the water cycle with warming. As atmospheric water vapor increases with temperature in line with Clausius-Clapeyron [*Allen and Ingram*, 2002; *Santer et al.*, 2007; *Willett et al.*, 2010], increasing transport of water from exporting to importing regions enhances existing patterns of precipitation minus evaporation (*P-E*) [*Held and Soden*, 2006]. A number of studies have shown that changes in precipitation or *P-E* are consistent with the WWDD paradigm at large scales in observations and models [e.g., *Liu et al.*, 2012; *Seager and Naik*, 2012; *Lau et al.*, 2013; *Liu and Allan*, 2013; *Chou et al.*, 2013; *Polson et al.*, 2013a; *Wu and Lau*, 2016; *Polson et al.*, 2016]; however, this pattern is expected to emerge more clearly over ocean than land [*Hegerl et al.*, 2015; *Byrne and O'Gorman*, 2015] and other studies find that the WWDD paradigm, for physical reasons, does not hold over land [*Greve et al.*, 2014; *Byrne and O'Gorman*, 2015; *Greve and Seneviratne*, 2015].

Part of the explanation behind these different conclusions regarding the validity of the WWDD paradigm may be related to changes in the location of the wet and dry regions over time due to unforced climate variability or forced circulation changes [*Chadwick et al.*, 2016]. While thermodynamically driven changes should lead to an increase in tropical precipitation, this is partly offset by dynamically driven changes which can have the opposite effect as the Walker cell weakens with warming [*Allan*, 2012; *Chadwick et al.*, 2013; *Bony et al.*, 2013; *Kent et al.*, 2015]. *Chadwick et al.* [2013] show that residual tropical spatial patterns of changing precipitation are dominated by the shifts in regions of convection and convergence. Poleward expansion of the Hadley cell and associated expansion of subtropical dry regions and shifts of the midlatitude storm tracks [*Seidel et al.*, 2008; *Seager et al.*, 2010; *Scheff and Frierson*, 2012] will also drive changes in precipitation.

Moreover, climatological differences between models mean that climate features are not necessarily colocated across simulations and observations. This can result in less agreement in precipitation trends between models than is found when these climatological differences are accounted for [*Levy et al.*, 2014; *Chadwick et al.*, 2016]. Furthermore, over land, water availability can also limit evaporation in dry regions, restricting changes in *P-E* and *Kumar et al.* [2015] show that this, along with unforced climate variability, can explain why different approaches to assessing the WWDD paradigm can produce apparently contradictory conclusions about its validity over land.

Here we analyze annual mean precipitation in tropical wet and dry regions in climate model simulations and satellite observations to investigate whether observed and modeled precipitation changes show decreasing precipitation in the dry regions and increasing precipitation in the wet regions. We investigate how the

mean wet and dry region precipitation changes are affected if we allow the regions to move in time compared to using regions that are fixed. We also investigate how the consistency between observations and models is influenced by the climatological discrepancies in models and observations. This is done by using four alternative methods to define the tropical (30°S–30°N) wet and dry regions.

Method (1) uses seasonally and interannually moving wet and dry region masks that track the shifting location of these regions over time and account for each simulation's own climatology.

Method (2) uses fixed annual masks derived from satellite observations' climatological annual mean precipitation, applied to all simulations (i.e., does not move seasonally or interannually).

Method (3) is the same as Method (2) but uses fixed annual masks derived from each simulation's own climatological annual mean precipitation.

Method (4) is the same as Method (2) but uses fixed seasonal masks derived from satellite observations' climatological seasonal mean precipitation (i.e., masks move seasonally but not interannually).

Method (1) accounts for seasonal and interannual changes in the location on the wet and dry regions, while Methods (2) and (3), both commonly used approaches, allow for differences in the climatological precipitation patterns between models to be investigated. Thus, the forced model precipitation changes will be more physically consistent than those obtained by simply averaging across all simulations, i.e., using Method (2), which may smear out changes. Method (4) allows us to investigate the affect of just accounting for the seasonal shifts in the location of the wet and dry regions, as *Chou et al.* [2013] and *Kumar et al.* [2015] show that the contrast between wet and dry seasons is also enhanced with warming. The paper will primarily focus on Methods (1) and (2) to compare the consistency in precipitation changes between models and observations using an approach that allows for differences in model climatology and shifts of wet and dry regions in the future versus an approach that defines fixed regions based on historical observations. Methods (3) and (4) then allow us to elucidate which of seasonality or changes in circulation are more important to account for. A perfect model detection and attribution analysis shows when the signal of external forcing is expected to emerge in the wet and dry regions over ocean and land for each of the 4 Methods.

2. Changes in the Wet and Dry Regions

2.1. Methods

Observations are from the satellite-based Global Precipitation Climatology Project (GPCP) gridded data set of monthly precipitation [*Adler et al.*, 2003] for the years 1988–2014 (for which Special Sensor Microwave/Imager measurements are available, making trends more reliable [*Hegerl et al.*, 2015]). Model data are from the Coupled Model Intercomparison Project Phase 5 archive [*Taylor et al.*, 2011]. Historical runs are combined with the RCP8.5 scenario runs to extend the analysis period from 1988 to 2100. Control runs are used to estimate the internal variability (Table S1 in the supporting information). Data are interpolated to the same 2.5° × 2.5° grid and tropical precipitation for 30°S–30°N is split into wet and dry regions using four methods. In each method the dry/wet regions are defined as the driest/wettest third of gridboxes.

Method (1) allows the wet and dry regions to move and defines them uniquely for the observations and each simulation for each season and year. The tropical mean precipitation, $\hat{P}_x(i,t)$, is the average precipitation in all dry or wet regions for season i and year t where x is *dry* or *wet*. Gridboxes are sorted from lowest to highest precipitation so that

$$\hat{P}_{\mathrm{dry}}(i,t) = \sum_{n=1}^{L_{1/3}} A_n P_n(i,t) \tag{1}$$

where P_n is the precipitation in gridbox n, $\hat{P}_{\mathrm{dry}}(i,t)$ is the mean precipitation for all gridboxes in the lower, L, 33.3 percentile ($n \in [1, L_{1/3}]$), for season i, year t, and A_n is an area weighting factor, similar to the approach used in *Liu and Allan* [2013] and *Polson et al.* [2013a]. $\hat{P}_{\mathrm{wet}}(i,t)$ is the mean precipitation of all gridboxes in the upper, U, third of gridboxes ($n \in [U_{1/3}, N]$), where N is the total number of gridboxes. Annual mean precipitation in year t and region x, $\hat{P}_{\mathrm{ANN},x}(t)$, is calculated by averaging over $\hat{P}_x(i,t)$ for all seasons, i, where seasons are January, February, and March (JFM), April, May June (AMJ), July, August, and September (JAS), and October, November, and December (OND). The moving masks were not found to move substantially from year to year or significantly over whole period, similar to the results shown in *Polson et al.* [2013a, Figure 1].

Method (2) uses a fixed annual mask for the wet and dry regions based on the GPCP observation's climatological mean annual precipitation for 1988–2014 (see Figure S1). The same fixed masks are applied to all

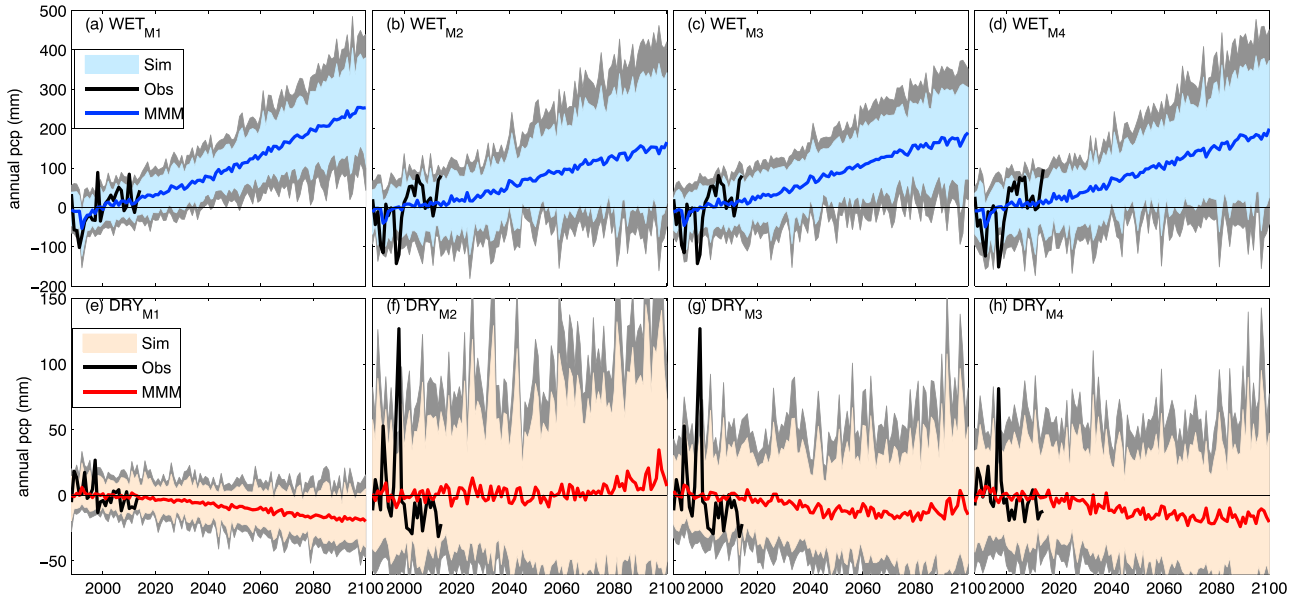

Figure 1. (a–d) Wet and (e–h) dry region tropical mean annual precipitation anomalies with respect to 1988–2014, (mm) for observations (GPCP) for 1988–2014 and models for 1988–2100. Wet and dry regions are defined using (Figures 1a and 1e) Method 1 (M1—unique moving masks for observations and each simulation), (Figures 1b and 1f) Method 2 (M2—the same fixed masks for observations and each simulation based on GPCP annual climatology), (Figures 1c and 1g) Method 3 (M3—unique fixed masks for observations and each simulation based their own annual climatology), and (Figures 1d and 1h) Method 4 (M4—the same fixed masks for observations and each simulation based on GPCP seasonal climatology). Sim (shaded) is 5%–95% range of all simulations (grey shading is double the model variance), MMM (blue and red lines) is multimodel mean, and Obs (black line) is observations.

simulations; thus, this method does not account for climatological biases in models or for shifts in location of the wet and dry regions with time. Therefore, in this case, we do not account for seasonal shifts in the wet and dry regions, and the mean tropical dry region annual precipitation is

$$\hat{P}_{\mathrm{ANN,dry}}(t) = \sum_{n=1}^{CL_{1/3}} A_n P_{\mathrm{ANN},n}(t) \tag{2}$$

where $P_{\mathrm{ANN},n}(t)$ is the mean annual precipitation in gridboxes ($n \in [1, \mathrm{CL}_{1/3}]$), where $[1, \mathrm{CL}_{1/3}]$ is the set of gridboxes in the lower 33.3 percentile based on climatological mean annual precipitation for all years. $\hat{P}_{\mathrm{ANN,wet}}(t)$ is the mean of gridboxes in the upper third of climatological mean annual precipitation, ($n \in [\mathrm{CU}_{1/3}, N]$).

In order to investigate the influence of the climatological differences between models and observations and also the influence of the seasonal shifts in the wet and dry regions, we also define the wet and dry regions using two further methods.

Method (3) uses an annual fixed mask for the wet and dry regions as in Method (2) but using each simulation's and the observation's own climatology, thus accounting for climatological differences in model and observational precipitation but not for shifts in the location of the wet and dry regions with time or seasons.

Method (4) is the same as Method (2) except that the fixed mask accounts for seasonal shifts of the wet and dry regions but not interannual shifts. Climatological precipitation from satellite observations for seasons JFM, AMJ, JAS, and OND is used to create a fixed mask that is applied to all years and all model simulations. Gridboxes in the wet and dry regions are identified for each season, and as in Method (1), the annual wet or dry precipitation is then calculated by averaging over all seasons.

2.2. Mean Precipitation Changes in Wet and Dry Regions

Figure 1 shows observed and model tropical mean wet and dry region annual precipitation anomalies for Methods (1)–(4). Using the moving wet and dry region masks that account for each simulation's own climatology (Method (1)) gives far better constrained estimates for future precipitation than using any of the fixed mask approaches (Methods (2)–(4)). The moving mask (Method 1—Figures 1a and 1e) gives consistently increasing precipitation in the wet regions and decreasing precipitation in the dry regions. In contrast, the observational-based annual fixed mask (Method 2—Figures 1b and 1f) has precipitation tending to increase in the dry regions toward the end of the 21st century.

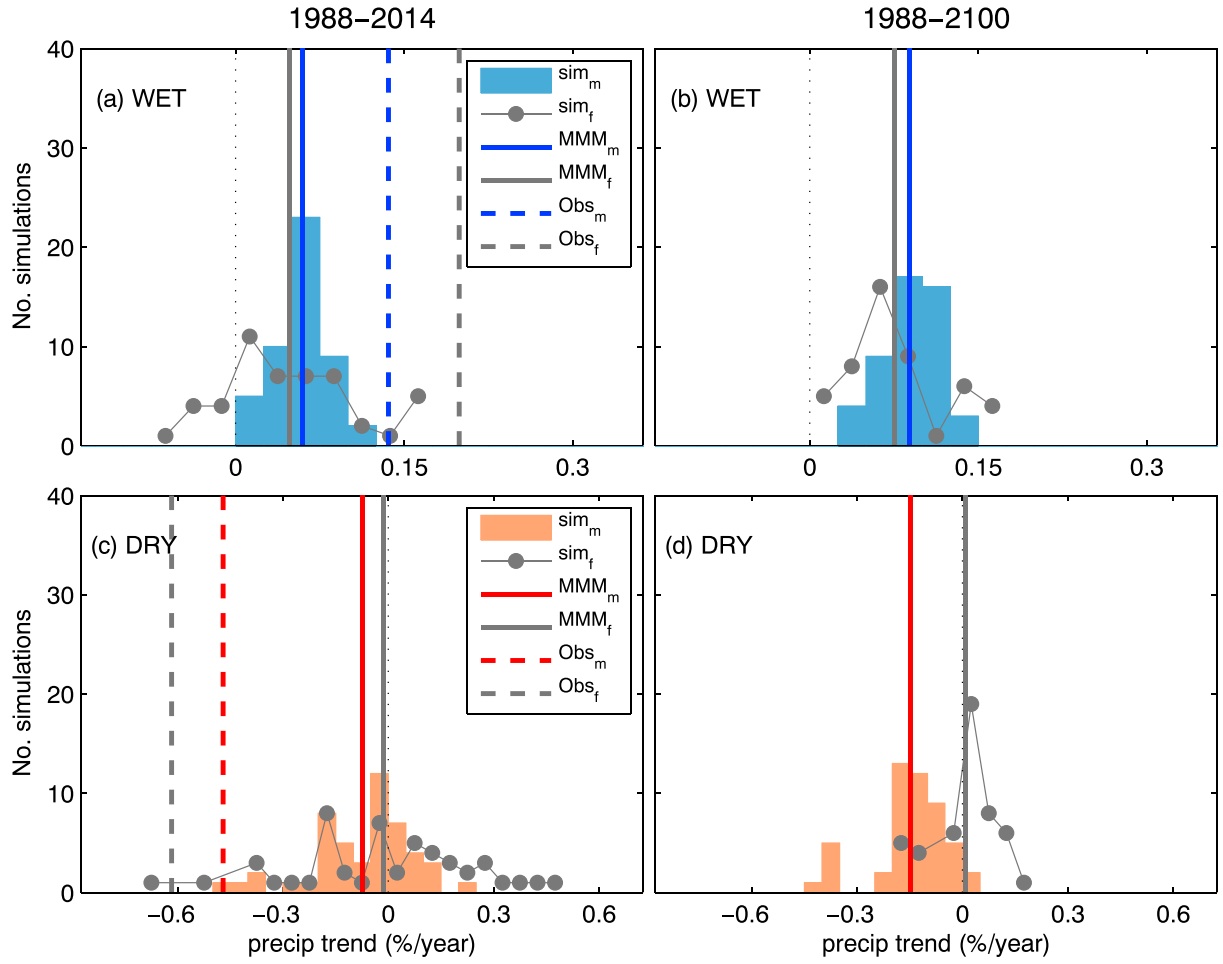

Figure 2. Distribution of simulated and observed trends in tropical mean annual precipitation (%/yr, with respect to 1988–2014) for 1988–2014 and projected trends for 1988–2100 for (a and b) wet regions and (c and d) dry regions. Trends are shown for unique moving wet/dry region masks (Method (1)) for observations (Obs_m) and each simulation (sim_m—shaded) and for the same fixed wet/dry region masks based on GPCP climatology (Method (2)) applied to observations (Obs_f) and simulations (sim_f—grey lines); MMM are multimodel means. Note the bars and dots on the line plots are directly comparable.

The multimodel mean spatial trends for 1988–2100 show the majority of the wet region gridboxes getting wetter and dry region gridboxes getting drier even with the observational-based fixed mask (Method 2, Figure S1). The observationally based mask may incorrectly identify the wet and dry regions in the model's own climatology which may be shifted compared to observations. However, as absolute precipitation changes are larger in wetter regions, the dry regions are more sensitive to the incorrect introduction of climatologically wetter regions than the wet regions are to the introduction of climatologically drier regions.

For the wet regions, accounting for each simulation's own climatology alone reduces the model spread (Method 3—Figure 1c) by 30% compared to Method (2), and the spread is similar, though slightly larger, than that from Method (1). Accounting for seasonality alone (Method (4)—Figure 1d) does not reduce the model spread compared to Method (2). For the dry regions, accounting for each simulation's own climatology alone reduces the model spread (Method 3—Figure 1g) by 30%, though the model spread is still much larger than that from Method 1 (by 67%). Therefore, allowing for the movement of the dry regions is important for reducing model uncertainty in tropical mean precipitation changes. Accounting for the seasonality alone (Method (4)—Figure 1h) also reduce the model spread by 30% compared to Method (2). The interannual variability of the observations is far larger using the fixed mask approaches (Methods (2)–(4)) compared to the moving mask (Method (1)), and the observations can substantially exceed the model spread in these cases.

The results for ocean only and land only show similar changes in the future, with the wet regions getting wetter and the dry regions getting drier when Method (1) is used to define the wet and dry regions. However, for the fixed mask approaches (Methods (2)–(4)), the dry regions do not show a robust drying trend

(Figures S2 and S3). This shows that particularly for the dry regions over land, accounting for circulation driven and seasonal changes in the location of the dry regions is important for detecting a drying signal [see also *Chou et al.*, 2013; *Kumar et al.*, 2015; *Hegerl et al.*, 2015].

Figure 2 compares the distribution of linear trends for Method (1) and Method (2), where a linear least squares regression was used to calculate the change in $\hat{P}_{ANN,x}(t)$ over all years, $\dot{P}_{ANN,x}$. Here $\dot{P}_{ANN,x}$ is expressed as a percentage relative to $\hat{P}_{ANN,x}(t)$ averaged over 1988–2014 to make the changes in the wet and dry regions more comparable. This shows that Method (1) provides more consistent trend estimates across simulations and better agreement between observations and models (Figures 2a and 2c) with a clear WWDD pattern across the vast majority of simulations for 1988–2100 (Figures 2b and 2d). The distribution of trends for Method (2) (and Methods (3) and (4), Figures S4 and S5) tends to be wider and does not show the drying of the dry regions as consistently across all simulations. In particular, drying of the dry regions is not seen for most simulations using Method (2); 69% of simulations have positive trends, compared to just 4% for Method (1). For Methods (3) and (4), the drying is also less consistent across simulations with 22% and 25% of simulations giving positive trends, respectively. There is also a better agreement between the observations and multimodel mean trends using the moving mask (Method (1)) than for any of the fixed mask approaches (Methods (2)–(4)). Nevertheless, the change in the observations is on the outer edge of the model range for each method.

3. Detection and Attribution

To determine if any method leads to earlier detection of the precipitation response to external forcing, we apply a standard total least squares detection and attribution analysis [*Allen and Stott*, 2003]. The analysis scales the multimodel mean forcing fingerprint, **F**, to best match observed precipitation changes, **y**. This is applied to the 1988–2014 time series of tropical mean annual precipitation anomalies for fingerprints $\hat{P}_{ANN,wet}(t)$ and $\hat{P}_{ANN,dry}(t)$. We apply the analysis to tropical mean precipitation over both land and ocean (land&ocean), ocean only, and land only.

$$\mathbf{y} = (\mathbf{F} + \varepsilon_{finger})\beta + \varepsilon_{noise} \tag{3}$$

where β is the scaling factor adjusting the magnitude of the fingerprint to fit the observations. Where $\beta > 0$, the forced fingerprint is detected in the observed changes, for $\beta > 0$ and <1 the fingerprint overestimates the observed changes, and for $\beta > 1$ the fingerprint underestimates the observed changes. ε_{noise} is the residual associated with internal variability and ε_{finger} is variability remaining in the fingerprint after multimodel averaging. Fingerprints are not optimized as uncertainty in the covariance introduces a further layer of complexity, and the focus here is the characterizing fingerprints.

To test the null hypothesis that the observations can be explained by internal variability alone, multiple samples of climate noise, estimated from model internal variability, are added to the noise-reduced $\tilde{\mathbf{F}}$ and $\tilde{\mathbf{y}}$ [*Allen and Stott*, 2003] and β is recalculated. If $\beta > 0$ at 5% significance level, then the fingerprint is detected in the observations [*Hegerl and Zwiers*, 2011]. Because models tend to underestimate observed variability in precipitation, particularly in the tropics [*Zhang et al.*, 2007; *Polson et al.*, 2013b, see also Figure 1], the model variance is doubled when calculating the noise samples.

The analysis is applied to the observations to investigate the detectability of external forcing in observed precipitation changes from 1988 to 2014. To assess when the fingerprint of external forcing is expected to become detectable, a perfect model study is applied to precipitation anomalies for 1988–2014, 1988–20XX, where XX is 25, 35, 45, 55, 65, 75, 85, and 95. In the perfect model study, each model simulation is used as pseudo-observations and the multimodel mean recalculated excluding that simulation before the detection and attribution analysis is applied. The percentage of the model ensemble where external forcing is detectable indicates the likelihood that forcing would be detectable in the observed changes.

3.1. Detection and Attribution of Observed Changes

The detection and attribution results for the observations for 1988–2014 show that external forcing is detectable for the wet regions but not the dry regions (Figure 3). This updated result is consistent with *Polson et al.* [2013a] which applied a similar analysis to satellite observations for 1988–2010. Using the moving mask (Method (1)) produces better constrained scaling factors than the fixed mask based on the observation climatology (Method (2)), consistent with the lower model spread seen in Figure 1. The scaling factors are also more consistent with the ideal value of "1" for the moving mask, demonstrating the better agreement between observations and models using this approach, but with models still significantly underestimating observed

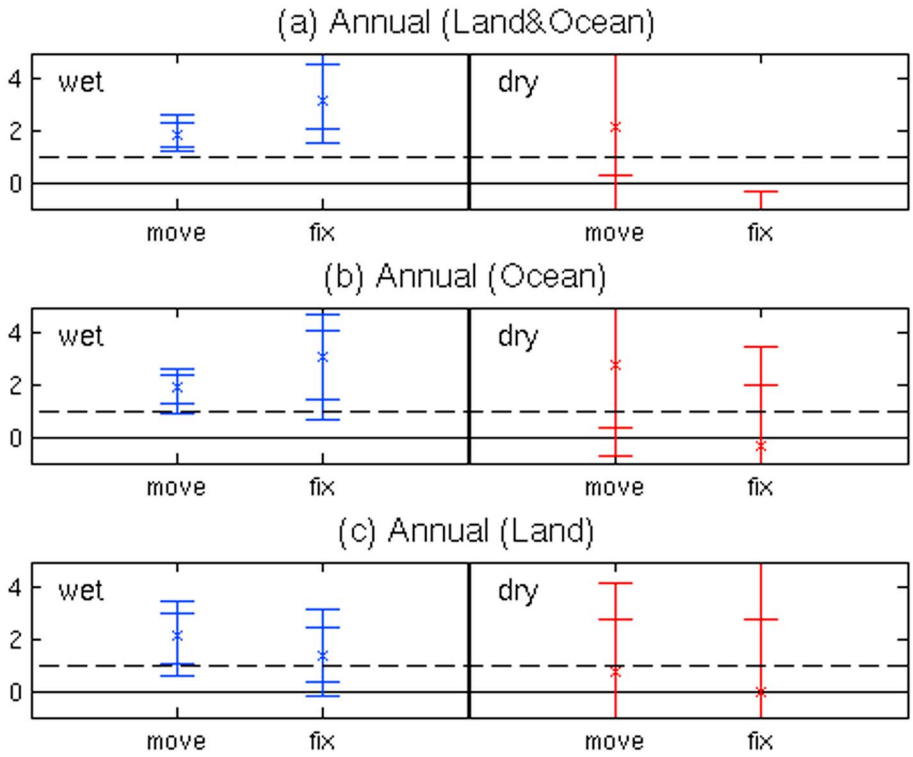

Figure 3. Detection results for the satellite data (GPCP) for tropical mean annual precipitation anomalies (from 1988–2014) for 1988–2014. Scaling factors (vertical axis) are shown for wet (blue) and dry (red) regions separately for (a) land and ocean, (b) ocean, and (c) land. Scaling factors are calculated using unique moving wet and dry region masks for observations and each simulation (move—Method (1)) and for the same fixed wet and dry region masks based on GPCP climatology (fixed—Method (2)) applied to observations and all simulations. Crosses are the best estimate scaling factor from the multimodel mean, and error bars show the 90% confidence interval for the raw and double the model variance.

changes as seen in Figure 2. External forcing is also detectable over land for the wet regions, but only if using the moving mask (Method (1)) and not for the fixed mask (Method (2)). The scaling factors for Methods (3) and (4) are similar to those of Method (2) (Figure S6), so accounting for just each simulation's own climatology or just the seasonal shifts of the wet and dry regions does not seem to significantly improve the detectability of observed changes in precipitation. This suggests that the interannual shifting of the wet and dry region is important for detecting external forcing.

3.2. Perfect Model Detection and Attribution Analysis

Figure 4 shows the percentage of pseudo-observations (simulations) for which external forcing should be detectable for each time window from 1988–2014 to 1988–2095. For both the wet and the dry regions, the moving mask (Method (1)) improves the detectability of external forcing compared to any of the fixed mask approaches (Methods (2)–(4)). For the wet regions, forcing is detectable in >90% of pseudo-observations for 1988–2014 and reaches 100% by 2035, consistent with our result of detectable changes in satellite data. For the fixed masks, the detectability rate is initially 50–70% and does not reach 100% until 2055 (Figure 4a). Method (3), which accounts for each models own climatology, is the second best method for wet regions. For the dry regions, the detectability rate starts low for all methods; however, for the moving mask (Method (1)), it exceeds 50% by 2045 and reaches >90% by 2065, while for the fixed mask methods it never exceeds 80% (Figure 4b). The annual fixed mask based on observed climatology (Method (2)) performs particularly poorly, never exceeding 50% detectability rate, which is unsurprising given the large model spread seen in Figure 1. This is due to the spurious inclusion of wetter regions which occurs due to differences in observation and models climatologies.

Results for ocean only are very similar to those for land and ocean. For land only the overall conclusions are similar, with the moving mask (Method (1)) providing significantly enhanced detectability compared to any of the fixed masks (Methods (2)–(4)). However, the detectability is generally lower for land than land and

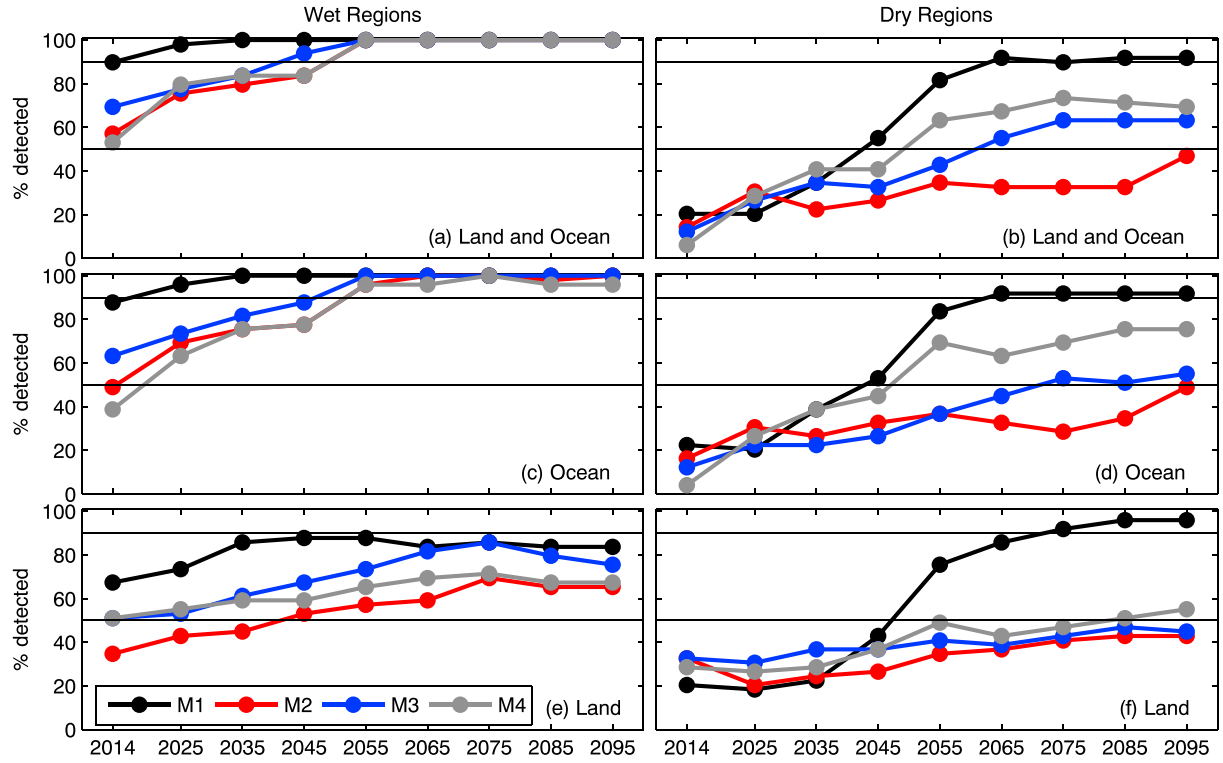

Figure 4. Percentage of pseudo-observations (simulations) where forcing is detectable from perfect model analysis for tropical mean annual precipitation anomalies (compared to analysis period) for 1988–2014, 2025, 2035, 2045, 2055, 2065, 2075, 2085, and 2095. Results are shown for wet and dry regions separately for (a and b) land and ocean, (c and d) ocean, and (e and f) land. Scaling factors are calculated wet and dry regions defined using Method (1) (M1—black), Method (2) (M2—blue), Method (3) (M3—red), and Method (4) (M4—grey).

ocean, as expected on physical grounds [e.g., *Byrne and O'Gorman*, 2015; *Hegerl et al.*, 2015] and consistent with publications questioning the WWDD paradigm [e.g., *Greve et al.*, 2014; *Greve and Seneviratne*, 2015]. The results are also in agreement with the detection and attribution analysis of observed precipitation changes (see section 3.2) which found that external forcing is detectable for wet regions but not the dry regions for 1988–2014 and that the models and observations are more consistent for the moving mask (Method (1)) compared to the fixed masks (Methods (2)–(4)).

4. Discussion and Conclusions

The results of the trend analysis for the wet and dry parts of the tropical circulation suggests a robust pattern of wet gets wetter and dry gets drier in the tropics over both land and ocean in observations and models for precipitation. While the physical basis for changes in the water cycle center on increased water vapor and amplification of *P-E* patterns with warming, our analysis focuses on the detectability of observed precipitation changes (observations of evaporation are lacking [*Hegerl et al.*, 2015]), which is more heterogeneous in space and time than evaporation but is subject to additional physical drivers such as local versus remote moisture availability. However, this WWDD signal is less consistent in models when the shifting locations of the wet and dry regions are not accounted for, particularly for the dry regions. Using a fixed wet and dry regions mask based on observed precipitation produces results that imply that there is more model disagreement in future tropical mean precipitation changes than may actually be the case. Accounting for each simulation's own climatology reduces the model spread by around 30%, implying that the correct mean state is important for projections. Also, the observed and perfect model detection and attribution results show that accounting for the movement of the wet and dry regions significantly improves the detectability of external forcing.

We find that external forcing is already detectable in observed wet region precipitation but that models may underestimate the magnitude of observed changes, consistent with the findings of a previous study that used a similar methodology but shorter observational record [*Polson et al.*, 2013a]. However, external forcing in observed precipitation changes in the dry regions cannot yet be detected. This is consistent with the results

of the perfect model study which suggest that the signal of external forcing is likely to be detectable for wet region precipitation for ocean only and land only for the period where observations are available (1988–2014). However, the influence of external forcing is unlikely to be detectable in the dry regions alone until around 2045 and only if model climatology and the shifting location of the dry regions is taken into account. Otherwise, we might erroneously conclude that external influence on dry region precipitation would not be detectable during the 21st century. An alternative approach to assessing the WWDD paradigm based on local climatology and accounting for evaporation is perhaps more appropriate for assessing future changes at the scale most relevant for impacts. Note that local projections of precipitation changes will not be improved by allowing the wet and dry regions to shift as this approach accounts for the circulation changes, which are one of the largest sources of uncertainty at these scales. However, when trying to detect and physically interpret the large-scale forced response of precipitation, accounting for climatological difference between models and circulation-induced shifts in the wet and dry region locations, may be more useful. This approaches reveals a remarkably more consistent precipitation response to forcing across models and crucially can significantly enhance the detectability of external forcing.

Acknowledgments
The authors thank Richard Allan and Susan Solomon for discussions and the data provider for the GPCP [*Adler et al.*, 2003]. We acknowledge the WCRP Working Group on Coupled Modeling, and we thank the climate modeling groups for making available their model output [*Taylor et al.*, 2011]. D.B. and G.H. are supported by the ERC funded project TITAN (EC-320691). G.H. was supported by NCAS and the Wolfson Foundation and the Royal Society as a Royal Society Wolfson Research Merit Award (WM130060) holder.

References

Adler, R., et al. (2003), The version 2 Global Precipitation Climatology Project (GPCP) monthly precipitation analysis (1979–present), *J. Hydrometeorol.*, *4*, 1147–1167.
Allan, R. P. (2012), Regime dependent changes in global precipitation, *Clim. Dyn.*, *39*(3–4), 827–840, doi:10.1007/s00382-011-1134-x.
Allen, M., and W. Ingram (2002), Constraints on future changes in climate and the hydrologic cycle, *Nature*, *419*(6903), 224–232.
Allen, M., and P. Stott (2003), Estimating signal amplitudes in optimal fingerprinting, Part I: Theory, *Clim. Dyn.*, *21*(5), 477–491.
Bony, S., G. Bellon, D. Klocke, S. Sherwood, S. Fermepin, and S. Denvil (2013), Robust direct effect of carbon dioxide on tropical circulation and regional precipitation, *Nat. Geosci.*, *6*(6), 447–451.
Byrne, M. P., and P. A. O'Gorman (2015), The response of precipitation minus evapotranspiration to climate warming: Why the wet-get-wetter, dry-get-drier scaling does not hold over land, *J. Clim.*, *28*(20), 8078–8092, doi:10.1175/JCLI-D-15-0369.1.
Chadwick, R., I. Boutle, and G. Martin (2013), Spatial patterns of precipitation 703 change in CMIP5: Why the rich don't get richer in the tropics, *J. Clim.*, *704*(2–3), 181–197.
Chadwick, R., P. Good, G. Martin, and D. P. Rowell (2016), Large rainfall changes consistently projected over substantial areas of tropical land, *Nat. Clim. Change*, *6*(2), 177–181.
Chou, C., J. C. H. Chiang, C.-W. Lan, C.-H. Chung, Y.-C. Liao, and C.-J. Lee (2013), Increase in the range between wet and dry season precipitation, *Nat. Geosci.*, *6*(4), 263–267.
Greve, P., and S. I. Seneviratne (2015), Assessment of future changes in water availability and aridity, *Geophys. Res. Lett.*, *42*, 5493–5499, doi:10.1002/2015GL064127.
Greve, P., B. Orlowsky, B. Mueller, J. Sheffield, M. Reichstein, and S. I. Seneviratne (2014), Global assessment of trends in wetting and drying over land, *Nat. Geosci.*, *7*(10), 716–721.
Hegerl, G., and F. Zwiers (2011), Use of models in detection and attribution of climate change, *Wiley Interdiscip. Rev. Clim. Change*, *2*(4), 570–591, doi:10.1002/wcc.121.
Hegerl, G. C., et al. (2015), Challenges in quantifying changes in the global water cycle, *Bull. Am. Meteorol. Soc.*, *96*(7), 1097–1115, doi:10.1175/BAMS-D-13-00212.1.
Held, I., and B. Soden (2006), Robust responses of the hydrological cycle to global warming, *J. Clim.*, *19*(21), 5686–5699.
Kent, C., R. Chadwick, and D. P. Rowell (2015), Understanding uncertainties in future projections of seasonal tropical precipitation, *J. Clim.*, *28*(11), 4390–4413, doi:10.1175/JCLI-D-14-00613.1.
Kumar, S., R. P. Allan, F. Zwiers, D. M. Lawrence, and P. A. Dirmeyer (2015), Revisiting trends in wetness and dryness in the presence of internal climate variability and water limitations over land, *Geophys. Res. Lett.*, *42*, 10,867–10,875, doi:10.1002/2015GL066858.
Lau, W. K.-M., H.-T. Wu, and K.-M. Kim (2013), A canonical response of precipitation characteristics to global warming from CMIP5 models, *Geophys. Res. Lett.*, *40*, 3163–3169, doi:10.1002/grl.50420.
Levy, A. A. L., M. Jenkinson, W. Ingram, and M. Allen (2014), Correcting precipitation feature location in general circulation models, *J. Geophys. Res. Atmos.*, *119*, 13,350–13,369, doi:10.1002/2014JD022357.
Liu, C., and R. P. Allan (2013), Observed and simulated precipitation responses in wet and dry regions 1850–2100, *Environ. Res. Lett.*, *8*(3), 034002.
Liu, C., R. P. Allan, and G. J. Huffman (2012), Co-variation of temperature and precipitation in CMIP5 models and satellite observations, *Geophys. Res. Lett.*, *39*, L13803, doi:10.1029/2012GL052093.
Polson, D., G. C. Hegerl, R. P. Allan, and B. B. Sarojini (2013a), Have greenhouse gases intensified the contrast between wet and dry regions?, *Geophys. Res. Lett.*, *40*, 4783–4787, doi:10.1002/grl.50923.
Polson, D., G. C. Hegerl, X. Zhang, and T. J. Osborn (2013b), Causes of robust seasonal land precipitation changes, *J. Clim.*, *26*, 6679–6697, doi:10.1175/JCLI-D-12-00474.1.
Polson, D., G. C. Hegerl, and S. Solomon (2016), Precipitation sensitivity to warming estimated from long island records, *Environ. Res. Lett.*, *11*(7), 074024.
Santer, B., et al. (2007), Identification of human-induced changes in atmospheric moisture content, *Proc. Natl. Acad. Sci. U. S. A.*, *104*, 15,244–15,253.
Scheff, J., and D. M. W. Frierson (2012), Robust future precipitation declines in CMIP5 largely reflect the poleward expansion of model subtropical dry zones, *Geophys. Res. Lett.*, *39*, L18704, doi:10.1029/2012GL052910.
Seager, R., and N. Naik (2012), A mechanisms-based approach to detecting recent anthropogenic hydroclimate change, *Nat. Geosci.*, *1*, 21–24.
Seager, R., N. Naik, and G. A. Vecchi (2010), Thermodynamic and dynamic mechanisms for large-scale changes in the hydrological cycle in response to global warming, *J. Clim.*, *23*(17), 4651–4668, doi:10.1175/2010JCLI3655.1.
Seidel, D. J., Q. Fu, W. J. Randel, and T. J. Reichler (2008), Widening of the tropical belt in a changing climate, *Nat. Geosci.*, *1*(1), 21–24.

Taylor, K. E., R. J. Stouffer, and G. A. Meehl (2011), An overview of CMIP5 and the experiment design, *Bull. Am. Meteorol. Soc.*, *93*(4), 485–498, doi:10.1175/BAMS-D-11-00094.1.

Willett, K. M., P. D. Jones, P. W. Thorne, and N. P. Gillett (2010), A comparison of large scale changes in surface humidity over land in observations and CMIP3 GCMS, *Environ. Res. Lett.*, *5*, 025210, doi:10.1088/1748-9326/5/2/025210.

Wu, H.-T. J., and W. K.-M. Lau (2016), Detecting climate signals in precipitation extremes from TRMM (1998–2013)—Increasing contrast between wet and dry extremes during the "global warming hiatus", *Geophys. Res. Lett.*, *43*, 1340–1348, doi:10.1002/2015GL067371.

Zhang, X., F. Zwiers, G. Hegerl, F. Lambert, N. Gillett, S. Solomon, P. Stott, and T. Nozawa (2007), Detection of human influence on twentieth-century precipitation trends, *Nature*, *448*(7152), 461–465.